FUDMA Journal of Sciences (FJS)
ISSN online: 2616-1370
ISSN print: 2645 - 2944
Vol. 8 No. 3, June, 2024, pp 56 - 65
DOI: https://doi.org/10.33003/fjs-2024-0803-2317

MASS-WASTING INDUCED SHIFTS OF THE BASE OF THE GAS HYDRATE STABILITY ZONE: EXAMPLES FROM THE OFFSHORE NIGER DELTA BASIN, NIGERIA

Muslim B. Aminu

Department of Earth Sciences, Adekunle Ajasin University Akungba-Akoko.

*Corresponding authors' email: muslimaminu@gmail.com; muslim.aminu@aaua.edu.ng

ABSTRACT

Mass-wasting episodes lead to significant changes in the pressure and temperature regimes within shallow marine sediments and induce variations in the thickness of the gas hydrate stability zone. These variations are marked by vertical migrations of bottom-simulating reflections that typically mark the base of the hydrate zone. Using exploration seismic data from the Offshore Niger Delta, this study presents two examples involving the vertical migration of the base of the gas hydrate stability zones induced by mass-wasting events. The first is related to a slope failure surface along the forelimb of an active thrust-cored anticline with considerable bathymetric relief. Sediment removal has induced both a decrease in overburden pressure and an incursion of cooler temperature flux in strata in the anticline and led to a migration of the base of the gas hydrate stability zone to deeper levels. The second case is related to a recent erosional event that has led to sediment removal along a seafloor channel course. Evidence of ongoing migration of the base of the gas hydrate stability zone to deeper levels is provided by the lateral termination of a BSR along channel wall, its absence beneath the channel bottom and its apparent downward bend close to the channel fringes. Apart from unroofing hydrate systems and releasing free gas into the ocean and possibly the atmosphere, mass-wasting events on the seafloor, represent significant drivers influencing the formation of gas hydrates in shallow subsea sediments and the thickness and depths of the gas hydrate stability zone.

Keywords: Mass-wasting, Gas hydrates, Bottom-simulating reflection, Gas hydrate stability zone, Niger Delta

INTRODUCTION

Gas hydrates (GH) are clathrates of water and gas, frequently methane, but also higher alkanes in some cases. They form in conditions of high pressure, low temperature and high salinity (Sloan and Koh, 2007: Collett, 2009). GH occur on land, beneath permafrost regions, and at sea, in shallow sediments along continental margins (Riboulot *et al.,* 2018). GH is considered a potential contributor to ocean acidification (Valentine *et al.,* 2001) and climate change (McGinnis *et al.,* 2006; Solomon *et al.,* 2009; Dickens 2003) due to methane gas release during GH dissociation, even though it is uncertain what amounts of methane released from GH dissociation reaches the atmosphere or what effects it might have on climate (Kesser, 2014).

Many factors influence gas hydrate stability in marine sediments and consequently can change the depth of the base of the gas hydrate stability zone (BGHSZ). These factors include pressure and temperature, gas composition and pore water salinity (Sloan 2003; Holder *et al.,* 1987; Collett, 2009), capillary forces (Daigle and Dugan, 2011), and the pore size and thermal properties of sediment (Clennell et al., 1999). GH stability can further be disrupted in an otherwise static hydrate system by several processes including (1) sudden and significant increases in water-bottom temperature, tectonic uplift, and rapid sedimentation (Bangs *et al.,* 2005, 2010; Foucher *et al.,* 2002; Zander *et al.,* 2017); (2) the rise of warm and high-salinity fluids through the GHSZ (Boswell *et al.,* 2012; Minshull & White, 1989; Taladay *et al.,* 2017; Tréhu *et al.,* 2004); and (3) changes in gas compositions (Andreassen *et al.,* 2000; Geletti & Busetti, 2011; Tinivella & Giustiniani, 2013) and the subsurface pressure regime (Pecher et al., 2017; Tinivella & Giustiniani, 2013). Such disturbances of the hydrate zone lead to changes in the thickness of the gas hydrate stability zone (GHSZ). These changes can influence the appearance of bottom-simulating reflections (BSRs) that mark the base of the hydrate sediments. Rising warm and high-salinity fluid lead to a shoaling of the BSR and the interruption of its otherwise continuous character (Chen *et al.,* 2012, 2014; Crutchley *et al.,* 2014; Hyndman & Davis, 1992; Pecher *et al.,* 2010). Other processes may produce multiple BSRs that are spatially collocated but occuring at different sub-bottom depths (Popescu *et al.,* 2006; Zander *et al.,* 2017). All these factors lead to vertical migrations of the BGHSZ.

Pressure and temperature changes exert the greatest influence on the migration of the BGHSZ (Sloan and Koh, 2007). Increasing pressure serves to increase the stability of GH and leads to a thickening of the BGHSZ and its migration to deeper depths. Increasing sub-bottom temperature serves to destabilize GH and thin the BGHSZ and thus shallow its base. The pressure effect is generally assumed to propagate to the GHSZ rapidly and influence the thickness of the GHSZ immediately (Bangs *et al,* 2005). The temperature effect on the other hand is believed to propagate to the BGHSZ over an extended period that could be up to 10000 years (Bangs *et al,* 2005). The temperature effect therefore lags the pressure effect in scenarios where both factors change. Increases in overburden pressure can result from sea-level rise and increased sedimentation due to mass wasting events (Ruppel, 2000; Davy *et al.,* 2010). This results in a thickening of the GHSZ and serves to move the BGHSZ to deeper levels. Conversely, tectonic uplift of the seafloor, sea-level drop and mass wasting events lead to decreased overburden pressures and serve to move the BGHSZ to shallower levels (Sloan and Koh, 2007; Ruffine *et al.,* 2013). Increases in ocean bottom-water temperatures and the accent of warm fluids from deep strata into the GHSZ raise the temperature of the shallow subsurface, destabilize GH and lead to a shoaling of the BGHSZ (Hyndman and Davis, 1992; Pecher *et al.,* 2010).

The migration of the BGHSZ is often evident in exploration seismic data with the development of double BSRs; a vertical or near vertical stacking of two or more BSRs (Posewang and Mienert, 1999; Matsumoto *et al.,* 2000; Foucher *et al.,* 2002; Baba and Yamada, 2004; Bangs *et al.,* 2005; Popescu *et al.,* 2006; Paganoni *et al.,* 2016). The shallower BSR is generally regarded as approximating the base of the current methane hydrates GHSZ while the deeper BSRs could represent the base of the biogenic hydrate stability zone in the climatic past, or the base of the thermogenic hydrate stability zone, or BSRs related to the sedimentary architecture of depositional elements and much more (Bangs *et al.*, 2005; Paganoni *et al.*, 2016). In situations where the GHSZ has shifted to deeper levels, the deeper BSR will approximate the current BGHSZ while the shallow BSR would indicate the previous BGHSZ (Kroeger *et al.,* 2023).

GH have been recovered from core from the seafloor of the Offshore regions of the Niger (Ruffine *et al.*, 2006) but their presence in shallow sediments in the Delta, has been mostly inferred from industry seismic data sets and seafloor sonar data (Hovland *et al.,* 1997; Brooks *et al.,* 2000; Cunningham and Lindholm, 2000; Sultan *et al.,* 2007, 2010, 2011; Aminu and Ojo, 2024). Aminu and Ojo, 2024, report the occurrence of four (4) double BSRs in the Offshore Niger Delta. This study presents two examples of the migration of BSRs believed to approximate the BGHSZ that are related to mass-wasting events from the Offshore Niger Delta region.

The Geology of the Study Area

The Niger Delta ranks among the most prolific Oil and Gas provinces in the world. Geographically, its limits are defined by latitudes 3˚N and 6˚N and longitudes 3˚E and 9˚E (Figure 1), and it extends across the southern coast of Nigeria into parts of Cameroon. It is delimited to the west and to the north by the Benin Flank and the by the Abakaliki High, respectively. Its limit eastwards is marked by the Calabar Flank. Offshore, the Dahomey Basin and the Cameroon Volcanic Line mark the western and eastern limits of the Delta, respectively. The sediment thickness contour of 2000 m or the 4000 m water depth is regarded at the offshore limit of the Delta (Weber and Daukoru, 1975; Tuttle *et al.,* 1999). The Niger Delta formed at the site of the triple junction occasioned by the separation of the African and South American continents and the opening of the South Atlantic Sea (Burke, 1972; Whiteman, 1982). Rifting was commenced in the Late Jurassic and continued through the Cretaceous (Lehner and De Ruiter, 1977; Tuttle *et al.*, 1999). The Niger Delta has five structural provinces that are the result of gravity-driven shale tectonics (Corredor *et al.,* 2005) (Figure 2): (1) a proximal extensional province hosting regional and sub-regional growth faults and controlled by downward and seaward movement of the basal shale sequence; (2) a diapiric province where faults planes provide opportunity for buoyant shales to reach shallow sediments; (3) the inner fold and thrust belt with an imbricated thrust system whose seafloor expression is an arcuate convex-to-sea ridge; (4) a detachment fold province with little deformation and; (5) the outer fold and thrust belt comprising two convex-to-sea lobes. The initial sedimentation across the Delta was constrained by the bathymetry of the oceanic crust below (Corredor *et al.,* 2005; Aminu and Ojo, 2018) while subsequent deformation has been the result of gravity and buoyancy-induced shale tectonics (Wu and Bally, 2000; Bilotti and Shaw, 2005; Corredor *et al.,* 2005). Strain resulting from the lateral motion of mobile shales beneath the extensional province is transferred seaward and results in buoyancy-induced diapiric motion of shales in the diapir province and compressional toe-thrust structures in the more distal regions of the Delta (Bilotti and Shaw, 2005; Corredor *et al.,* 2005). Significant though lesser influences have been exerted by sea level variations and the rate of sediment supply, on the development of the Delta (Doust and Omatsola, 1990). Maximum water depth in the Offshore Niger Delta is greater than 4000 m (Tuttle *et al.,* 1999).

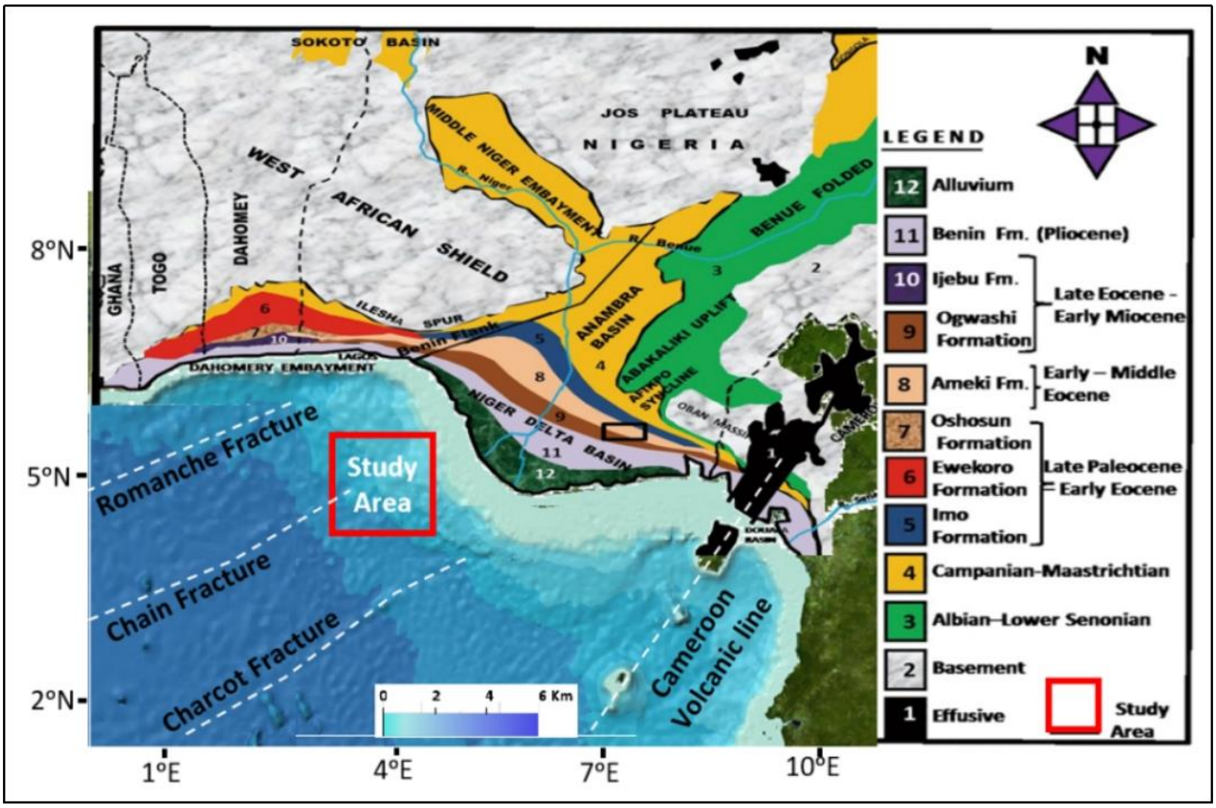

Figure 1: Bathymetric image of the Niger Delta highlighting major structural elements and province outline (modified after Adeleye *et al.,* 2020 and Aminu and Ojo, 2021)

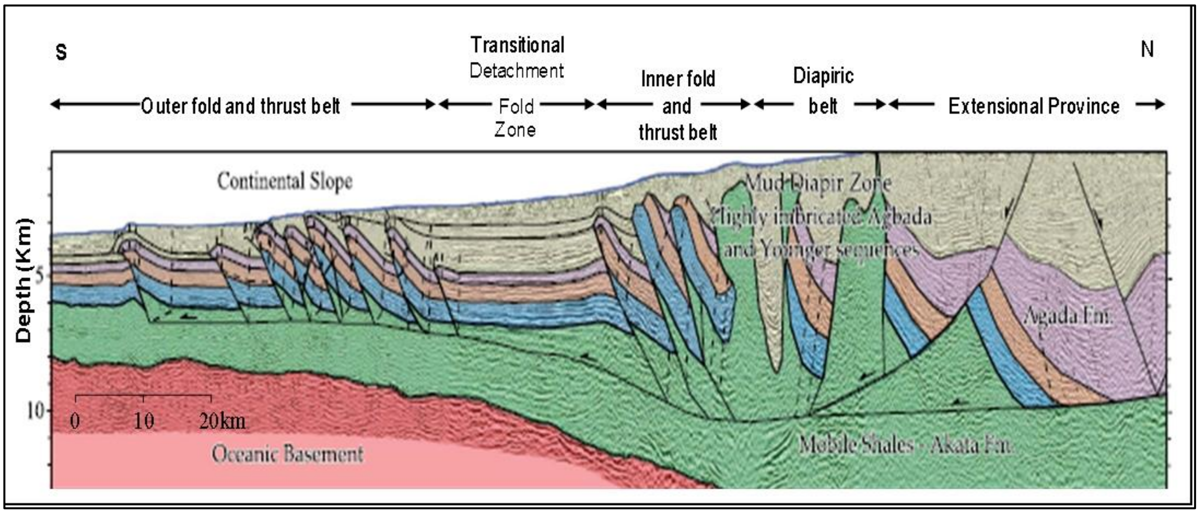

Figure 2: Structural provinces of the Niger Delta. Sediment collapse on the continental shelf leads to diapiric shale movement and toe-thrust structures in the more distal portions of the Delta (adapted from Corredor *et al.,* 2005)

The Niger Delta Basin consists of three stratigraphic units; the Akata, Agbada and Benin Formations (Frankl and Cordry, 1967; Short and Stauble, 1967; Avbovbo, 1978; Reijers, 2011). The Akata Formation is at the base of the stratigraphic succession and comprises of transgressive marine shales. Syn-rift clastic fragments of the oceanic basement below possibly underlie the Akata Formation (Corredor *et al.,* 2005; Sahota, 2006) (Figure 3). It is considered the major source rock of the Delta. The Agbada Formation is a faulted sequence of intercalated continentally derived sands and transgressive marine shales. The Agbada Formation overlies the Akata Formation (Avbovbo, 1978). It is the dominant reservoir rock in the Delta, and its shale intercalations are regarded as a potential second source of hydrocarbons (Nwachukwu and Chukwura, 1986). The Benin Formation is the youngest of the Niger Delta sequences. It overlies the Agbada Formation and consists of massive, porous and usually unconsolidated, fresh-water continental sands (Avbovbo, 1978; Reijers, 2011). The Benin Formation is absent in the most distal deepwater sections of the Delta (Cobbold *et al.,* 2009; Maloney *et al.,* 2010).

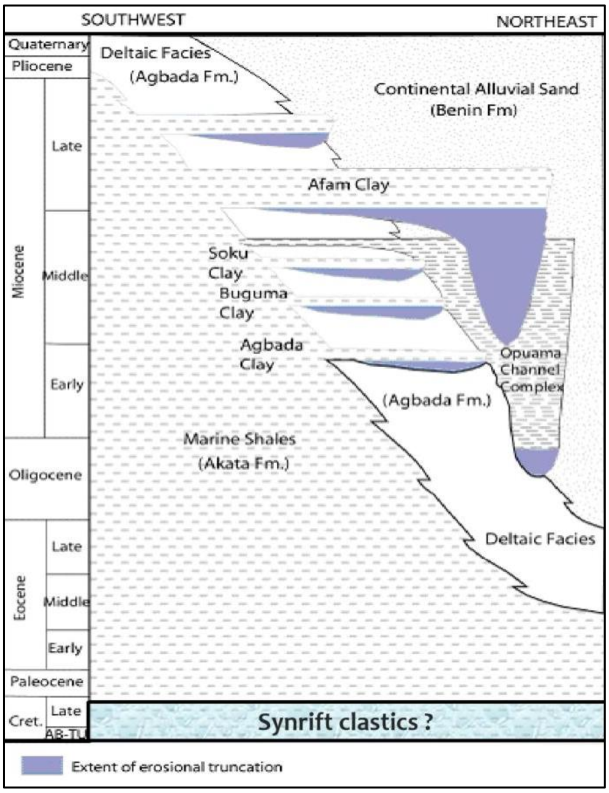

Figure 3: Stratigraphic column of the three conformable formations of the Niger Delta (Modified from Tuttle *et al.,* 1999)

The study area is located in the Western Niger Delta in water depths generally in excess of 1000 m (Figure 4a). This area hosts the seafloor expressions of the most westerly extensions of both the inner and the outer fold and thrust belts, with multiple seafloor thrust-cored ridges whose axes trend in the NNW-SSE (for the inner) and NW-SE (for the outer) directions, respectively. The general bathymetric dip in the area is in the southwest direction. Two seafloor channels traverse the area and follow the southwesterly dip of the seafloor. Near thrust ridges, the channels take advantage of saddles in the relay ramps between aligned thrust ridges to maintain an essentially linear course. Indications exist that the more northwesterly channel predates the second channel (Figure 4b).

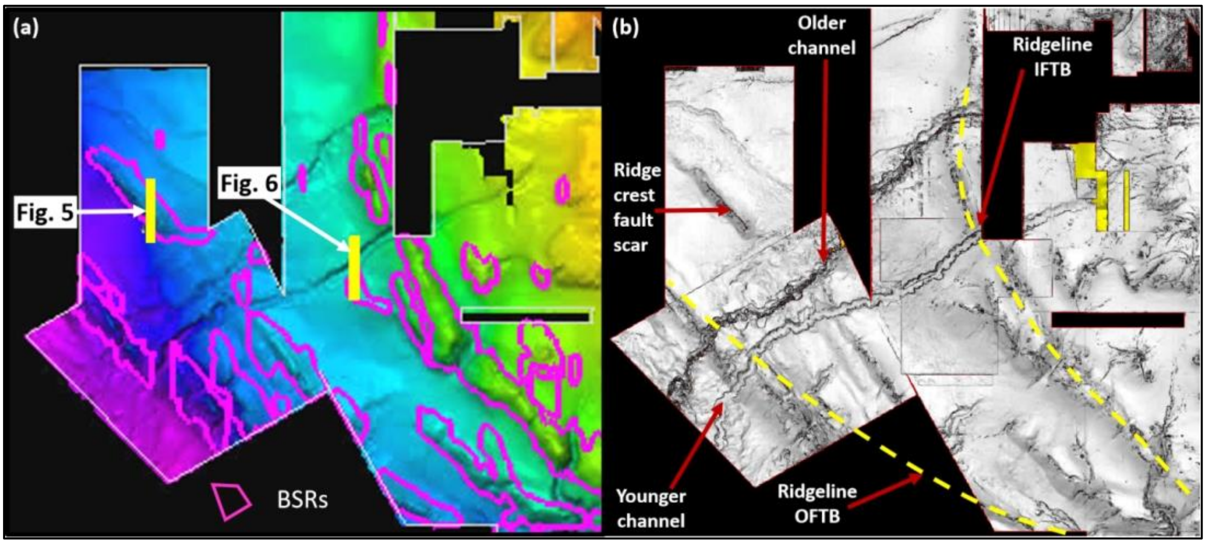

Figure 4: Seafloor bathymetric image of the study area. (a) Time structure map, (b) Chaos image. (Modified from Aminu and Ojo, 2024). The Chaos image indicates a greater reworking of the thalweg of the older channel relative to the younger one. IFTB = Inner fold and thrust belt. OFTB = outer fold and thrust belt. See Figure 1 for the location of the study area

MATERIALS AND METHODS

The data used in this study came from a 3D digital seismic merge actualized from independent oil and gas exploration seismic surveys that had been acquired over decades of exploration in the Offshore Niger Delta region. Individual seismic surveys comprising the data merge were acquired at different times and with varying acquisition parameters. These surveys had been rep-processed over time with updated and improved processing sequences and algorithms (Aminu and Ojo, 2024). The digital seismic merge was generally of high resolution with the exception of a few anticlinal structures where the cores of the faulted structures are poorly illuminated due as a result of variations in seismic resolution and noise suppression quality from individual surveys that make up the data merge. Data coverage was is roughly 79,000 sq km and record length was 8400 ms. The seismic interpretation was carried out in Petrel. For approximate depth estimation, a velocity of 1480 ms^{-1} (Maloney *et al.*, 2010) was used for the water column.

RESULTS AND DISCUSSION

Seismic indications of shifts in the BGHSZ are interpreted from the deep Offshore regions of the Western Niger Delta by tracking double bottom-simulating reflectors. The shifts are identified to be related to the two mass-wasting events, (i) a slope failure on a thrust-cored anticline and; (ii) a recently eroded seafloor channel.

(i) **Thrust-cored anticline slope failure**: In the western region of the study area, in water depths greater than 2300 m (>3200 ms *twt*), a thrust-cored anticline with an axial trend in the NW-SE direction hosts a slope failure on its seaward face. The axial span and anticline width are about 35 km and 7 km, respectively ((Figure 4a). A N-S section across the anticline (Figure 5) indicates a failure surface represented by a flat seaward limb with a constant dip of roughly 50°. Arched-up strata in the crest of the anticline terminate laterally along this failure surface. In the anticline, two (2) vertically-stacked bottom-simulating reflections are visible and can be tracked through the data for several kilometers along the anticline. Both BSRs exhibit reverse polarity reflection character relative to the seafloor reflection. The upper BSR dips at a considerable angle (likely greater than 25°) in the landward direction and nearly terminates laterally at the slope failure surface along with sediment strata in the apex of the anticline. The deeper BSR cut across arched upper strata in the anticline and occurs at as much as 300 ms (*twt*) beneath the upper BSR, particularly in the region of the failure surface. The two BSRs appear to converge in a 'weld' region in the back limb of the thrust-cored anticline before soling out to flat-lying strata further to the north. Seismic amplitude dimming occurs above the upper BSR and in the region between the two BSRs. Closer to the region of the weld, seismic amplitudes are greater in the space between the two BSRs. The upper BSR further exhibits greater amplitudes and higher lateral continuity in the back-limb region closer to the weld. In the regions proximal to the failure surface, the upper BSR is more discontinuous and of lower amplitudes. Enhanced amplitude reflections occur beneath the deeper BSR.

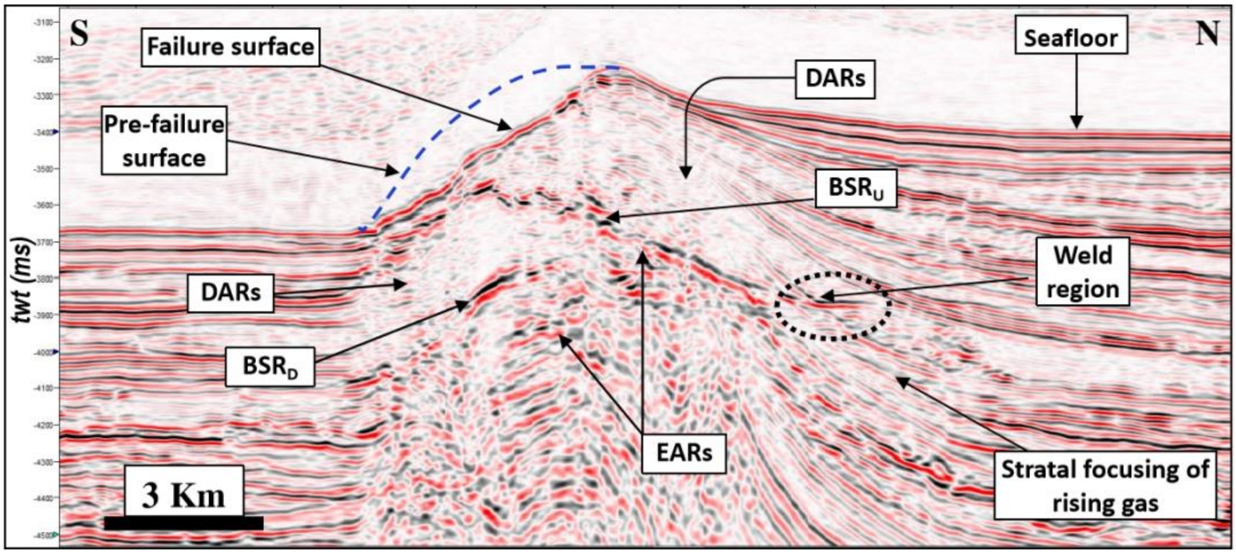

Figure 5. N-S Seismic line through the thrust-cored anticline. The slump failure has resulted in a flat forelimb for the thrust anticline. Two BSRs, BSR_U and BSR_D indicate the positions of the BGHSZ in the recent past and present. See Figure 4 for spatial location.

(ii) **Recently Eroded Seafloor Channel**: In the central region of the study area, in water depths greater than 1850 m (>2500 ms *twt*), a recently eroded seafloor channel runs more than 100 km across the study area in the NE-SW direction (Figure 6). The channel is linear and shows little evidence of avulsion. In plan view, its thalweg is smooth and shows little signs of cut-and-fill structures indicating it is a recently eroded channel compared to its neighbor, slightly northwestward, a second channel with more a chaotic thalweg (Figure 4b). The channel width is more than 1000 m. A N-S section along the channel reveals a channel with multiple cut and fill trenches: apparently, an initially broad cut and fill groove of the channel with an asymmetric U-shaped cross-sectional geometry, has been re-eroded along two separate axes that have produced two embedded V-shaped cross-sectional grooves. On the seaward southern side of the channel, multiple normal faults that reach the seafloor, sole to a detachment level that appears coincident with a BSR extending laterally southwards from the channel fringes for more than 3 km. Faulted blocks between these normal faults are rotated in a clockwise sense that indicates a southward slip along the detachment. The BSR is a strong reverse polarity reflection (relative to the seafloor reflection) with strong amplitude and lateral continuity cutting across sediment stratification. At the southern fringe of the channel wall, the BSR is slightly depressed to deeper levels before becoming indistinguishable from sediment stratification. The northern projection of this BSR is difficult to identify due to the presence of a thick mass-transport deposit (MTD). The BSR is likely represented here by a strong seismic reflection at the base of the MTD. South of the channel, though the MTD is visible, it is much thinner and occurs at a level much higher than the BSR. This entire system sits above a sedimentary succession defined at depth by rotated fault blocks bounded by blind normal faults within the apex of a broad and gently dipping anticlinal structure. An extensive erosional surface defines the upper limit of this anticline. Southwards of this erosional surface indications of a deeply eroded paleo-channel exist. This channel has an asymmetric V-shaped cross-sectional morphology.

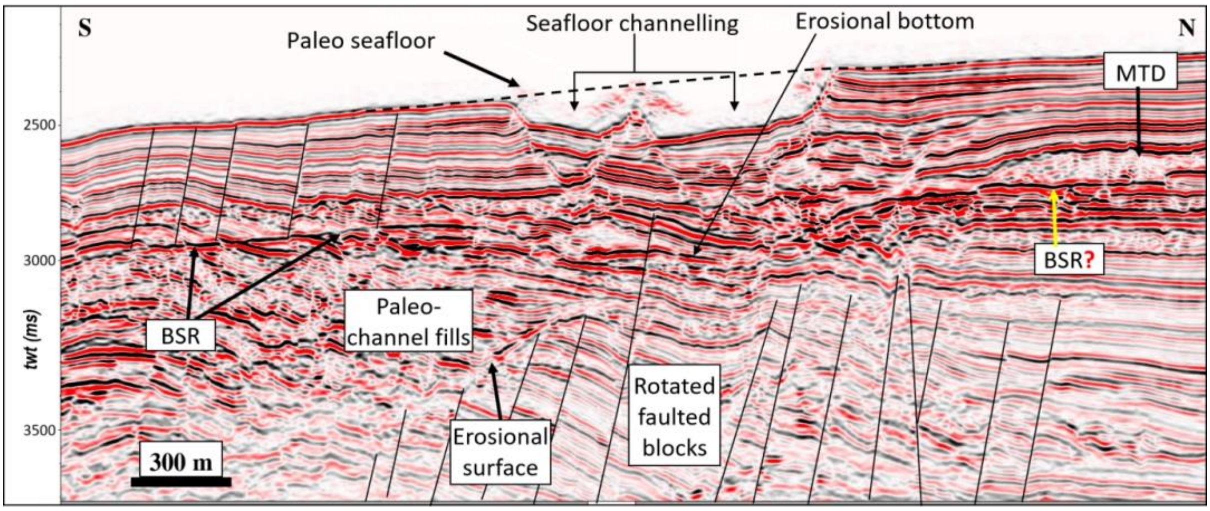

Figure 6: N-S Seismic line through the recently eroded channel. See Figure 4 for spatial location. The original asymmetric U-shaped channel morphology has been filled and re-eroded along two separate V-shaped trenches. Normal fault sloe to the BSR on the southern side of the channel while an MTD possibly sits atop the same BSR north of the channel axis.

Discussion

Figure 7 is a schematic model of the subsurface disposition beneath the thrust-cored anticline presented in Figure 5. The slope failure has removed sediments from the forelimb of the anticline and has induced migration of the initial BGHSZ to deeper levels. Pressure and temperature conditions are important drivers of the stability of GH in shallow subsea sediments (Sloan and Koh, 2007; Zander *et al.,* 2017). A reduction in lithostatic pressures as a result of sediment removal leads to instability of GH within the GHSZ and results in a decrease in the thickness of the GHSZ. This forces a dissociation of GH at the BGHSZ and its migration to shallower levels. BSRs approximating the BGHSZ therefore tend to migrate upward to shallower levels where equilibrium conditions exist (Haacke *et al.,* 2009). The pressure effect is believed to be instantaneous and occurs immediately after the reduction in pressure gradient induced by the slope failure (Bangs *et al.,* 2005). Conversely, a lowering of temperature in shallow sediments within the failed anticline occasioned by the incursion of cooler bottom waters along the slope failure surface would result in increased GH stability within the thrust-cored anticline, forcing a migration of the BGHSZ to deeper levels. This temperature effect operates on a longer time scale relative to the pressure effect and could require a propagation time of up to 10000 years (Bangs *et al.*, 2005; Zander *et al.,* 2017). In the case of this slope failure, temperature changes propagating to deeper levels within the thrust-cored anticline apparently have reached beyond the upper BSR so as to cause GH dissociation at its location and induce a migration of the BGHSZ to deeper depths as defined by the position of the deeper BSR. This likely explains the discontinuous signature of the upper BSR in the region proximal to the slope failure surface. The more continuous nature of the upper BSR in the region of the weld possibly indicates that the temperature flux front created by the slope failure is yet to reach the region of the weld. The dimmed seismic amplitudes possibly indicate the presence of some GH both above the upper BSR and in the intervening section between the two BSRs, particularly close to the failure surface. The higher amplitudes in the intervening space between the BSRs closer to the weld region possibly indicate the presence of free gas in this region. High amplitude reflections beneath the deeper BSR could indicate the presence of free gas beneath the newly formed BGHSZ accumulated from focused flow along dipping sediment strata deeper in the sedimentary succession.

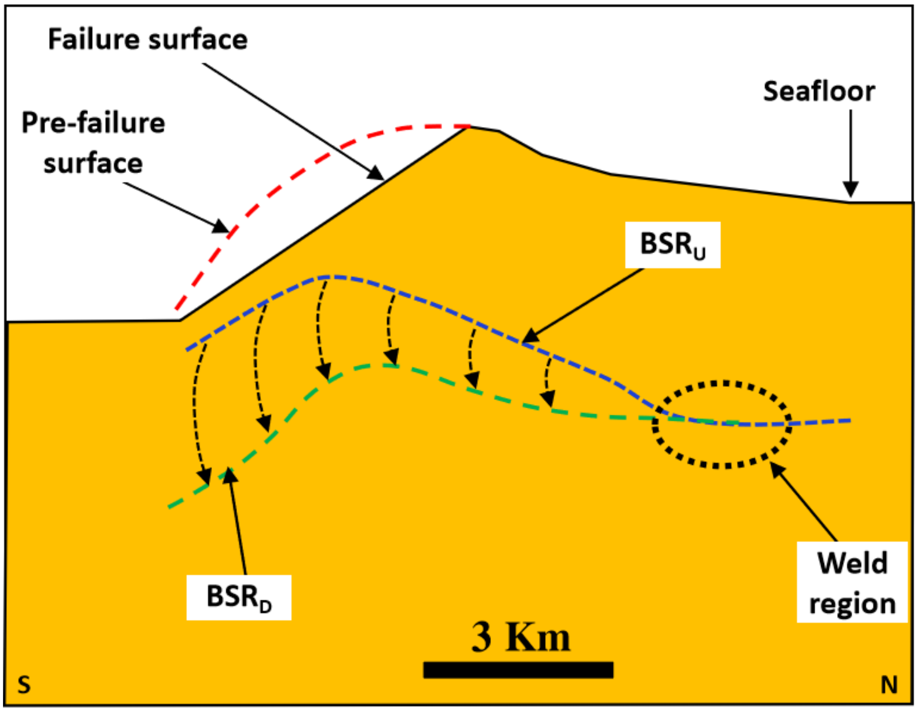

Figure 7: Schematic cross-section through the thrust-cored anticline shown in Fig. 5. A downward propagating cool front has deepened the depth of the BGHSZ beneath the thrust-cored anticline and a new BSR (BSR_D) is forming beneath the initial BGHSZ defined by BSR_U. Apparently, the process is ongoing and both BSRs are in a state of thermal disequilibrium.

Figure 8 is a schematic model of the N-S section across the channel presented in Figure 6. Channel erosion along the course of the channel has resulted in the removal of hydrate-bearing sediment and possibly enabled the escape of free gas from beneath the GHSZ. This is indicated by the lateral terminal of the BSR close to the channel wall. This BSR occurs at a much shallower depth than the initial asymmetric U-shaped channel eroded along the channel course and its lateral projections along the channel would have been removed during the erosional event that led to the channel. The removal of sediments along the channel course and the attendant reduction in overburden pressure normally serve to migrate the BGHSZ to shallower levels. However, this effect cannot occur as no sediments remain at the channel location beyond the initial erosion of the U-shaped channel. The incursion of cooler sub-bottom waters along the channel course would have served to reduce temperatures in sediments beneath the channel bottom and encourage a thickening of the GHSZ. The BGHSZ there would therefore migrate to deeper levels beneath the channel thalweg. Apparently, this process is still ongoing since no BSR is observed beneath the channel bottom. The BGHSZ is still in thermal disequilibrium and a BSR making it is yet to form. However, this ongoing migration of the BGHSZ to deeper levels beneath the channel course is indicated in the downward bend of the BSR close to the channel fringes. It can be expected that when the BGHSZ reaches thermal equilibrium and becomes quasi-static, a BSR approximating its location will form in the channel fills that occupied the initially eroded section. The BSR would describe a sagged trajectory beneath the channel course relative to the BSR south of the channel. Such undulating BSRs have been reported in the literature and have been adduced to be the result of differential thermal fluxes along their trajectory (Aminu and Ojo, 2021).

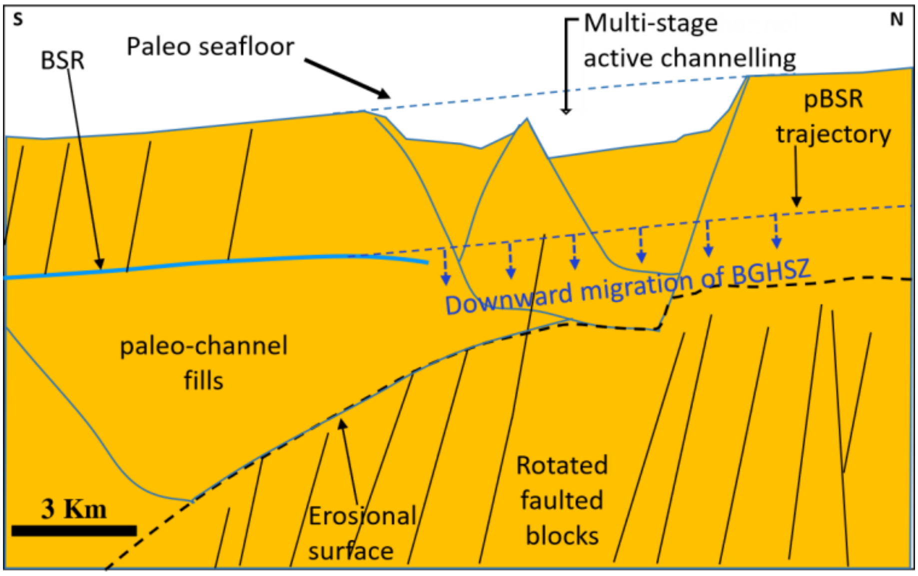

Figure 8: Schematic cross-section through part of the seismic line shown in Fig. 6. Channel erosion beyond the depth of the BSR apparently has removed hydrated sediments and unroofed free gas beneath the BGHSZ. Thus a BSR is absent beneath the channel course. The downward bend of the northernmost end of the BSR indicates a process of downward recalibration of the BSR beneath the channel and in regions proximal to the channel axis.

Mass-wasting events such as slope failures and seafloor channel erosion, represent important factors influencing the dissociation of GH in shallow sediments, the thickness of the GHSZ and the dynamic movements of the BGHSZ. Further, they are important factors influencing the rate of release of free gas into the ocean and ultimately the atmosphere, whether it be free gas trapped beneath the BGHSZ or free gas resulting from the dissociation of GH within the BGHSZ. They therefore represent a potentially significant influence on the local rates of ocean acidification and also climate change. Such events should, therefore, be taken into account when modeling methane release impacts on global climate.

CONCLUSION

Two examples of shifts in the base of the gas hydrate stability zone from the Offshore Niger Delta have been presented in this study. The shifts are related to mass-wasting events, specifically, a slope failure event on the forelimb of a thrust-cored anticline and a recently eroded channel course. Drastic changes in the pressure and temperature regimes in shallow sediments related to the mass-wasting events are adduced as the key drivers for the destabilization of gas hydrates within the gas hydrates stability zone and the consequent migration of the base of the zone to deeper levels. Significant sediment removal accompanying both the slope failure and the erosion along the seafloor channel served to both reduce overburden pressures and enable the influx of cooler sub-bottom water into sub-bottom sediments. The change in pressure and temperature in the shallow subsurface induced destabilization and dissociation of GH within the GHSZ and forced the BGHSZ to seek a new equilibrium depth at deeper levels. In both mass-wasting events presented in the study, the BGHSZs are yet to fully attain a new equilibrium state though the slope failure case is evidently more complete than the channel erosion situation. Mass-wasting events, therefore, represent a key process affecting the rate of gas hydrate dissociation in shallow subsea sediments and the release of free gas into the ocean and atmosphere, and are potential factors in ocean acidification and climate change. Accounting for the impact of mass-wasting events in climate modeling should lead to more reliable climate models.

ACKNOWLEDGEMENTS

I am grateful to the Nigerian Upstream Petroleum Regulatory Commission, Nigeria, and Chevron Nigeria Limited, for providing data for this study. This research did not receive any specific grant from funding agencies.

REFERENCES

Adeleye, M. A., Yekeen, K. O. & Amidu, S. A. 2020. Seismic stratigraphic analysis for hydrocarbon exploration in the Beta Field, Coastal Swamp Depobelt, Niger Delta. Geology, Geophysics & Environment. 46 (4): 259–271. https://doi.org/10.7494/geol.2020.46.4.259

Aminu, M. B. & Ojo, S. B. 2018. Application of spectral decomposition and neural networks to characterise deep turbidite systems in the outer fold and thrust belt of the Niger Delta. Geophysical Prospecting. https://doi.org/10.1111/1365-2478.12569.

Aminu, M. B. & Ojo, S. B. 2021. Multiple Bottom Simulating Reflections in the Deepwater Niger Delta: Seismic Character and Inferred Gas Supply Dynamics. International Journal of Scientific Research and Engineering Development. 4(3), 316-327.

Aminu, M. B. & Ojo, S. B. 2024. Seafloor Morphology and Potential Gas Hydrate Distribution in the Offshore Niger

Delta. International Journal of Advanced Geosciences, 12(1), 17-26.

Andreassen, K., Mienert, J., Bryn, P. & Singh, S. C. 2000. A double gas hydrate related bottom simulating reflector at the Norwegian continental margin, in: Holder G. D., Bishnoi, P. R., (Eds.), Gas Hydrates: Challenges for the Future, Annals of the New York Academy of Science 912, 126-135. https://doi.org/10.1111/j.1749-6632.2000.tb06766.x

Avbovbo, A.A. 1978. Tertiary lithostratigraphy of Niger Delta. American Association of Petroleum Geologist Bulletin 62, 295-306. https://doi.org/10.1306/C1EA482E-16C9-11D7-8645000102C1865D .

Baba, K. & Yamada, Y. 2004. BSRs and associated reflections as an indicator of gas hydrate and free gas accumulation: an example of accretionary prism and forearc basin system along the Nankai Trough, off central Japan. Resource Geology 54, 11-24. https://doi.org/10.1111/j.1751-3928.2004.tb00183.x

Bangs, N. L. B., Musgrave, R. J. & Trehu, A. 2005. Upward shifts in the southern Hydrate Ridge gas hydrate stability zone following postglacial warming, offshore Oregon. Journal of Geophysical Research 110, B03102. https://doi.org/10.1029/2004JB003293

Bangs, N. L., Hornbach, M. J., Moore, G. F. & Park, J.-O. 2010. Massive methane release triggered by seafloor erosion offshore southwestern Japan. Geology 38, 1019-1022. https://doi.org/10.1130/G31491.1

Bilotti, F. & Shaw, J. H. 2005. Deep-water Niger Delta fold and thrust belt modeled as a critical-taper wedge: The influence of elevated basal fluid pressure on structural styles. American Association of Petroleum Geologist Bulletin 89, 1475–1491. https://doi.org/10.1039/C0EE00203H .

Boswell, R., Collett, T. S., Frye, M., Shedd, W., McConnell, D. R., & Shelander, D. 2012. Subsurface Gas Hydrates in the Northern Gulf of Mexico. Mar. Pet. Geology. 34 (1), 4–30. https://doi.org/10.1016/j.marpetgeo.2011.10.003

Brooks, J. M., Bryant, W. R., Bernard, B. B. & Cameron, N. R. 2000. The nature of gas hydrates on the Nigerian Continental slope. Annals of the New York Academy of Sciences 912, 76 - 93

Burke, K., 1972. Longshore drift, submarine canyons and submarine fans in development of Niger Delta: American Association of Petroleum Geologist Bulletin 56, 1975-1983. https://doi.org/10.1306/819A41A2-16C5-11D7-8645000102C1865D .

Chen, L., Chi, W. C., Liu, C. S., Shyu, C. T., Wang, Y. & Lu, C. Y. 2012. Deriving regional vertical fluid migration rates offshore southwestern Taiwan using bottom-simulating reflectors. Marine Geophysical Research, 33(4), 379–388. https://doi.org/10.1007/s11001-012-9162-4

Chen, L., Chi, W. C., Wu, S. K., Liu, C. S., Shyu, C. T., Wang, Y. & Lu, C. Y. 2014. Two dimensional fluid flow models at two gas hydrate sites offshore southwestern Taiwan. Journal of Asian Earth Sciences, 92, 245–253. https://doi.org/10.1016/j.jseaes.2014.01.004

Clennell, M.B., Hovland, M., Booth, J.S., Henry, P. & Winters, W.J. 1999. Formation of natural gas hydrates in marine sediments: 1. Conceptual model of gas hydrate growth conditioned by host sediment properties. Journal of Geophysical Research. Solid Earth, 104 (B10), 22985–23003. https://doi.org/10.1029/1999JB900175

Cobbold, P. R., Clarke, B. J. & Løseth, H. 2009. Structural consequences of fluid overpressure and seepage forces in the outer thrust belt of the Niger Delta. Petroleum Geoscience 15, 3–15. https://doi.org/10.1144/1354-079309-784

Collett, T. S. 2009. Gas Hydrate Petroleum Systems in Marine and Arctic Permafrost Environments. In Carr et al., (Eds). Unconventional Energy Resources: Making the Unconventional Conventional: 29th Annual GCSSEPM Proceedings. Houston, Texas: Gulf Coast Section of the Society of Economic Paleontologists and Mineralogists Foundation, 6–30. https://doi.org/10.5724/gcs.09.29.0006

Corredor, F., Shaw, J. H. & Bilotti, F. 2005. Structural styles in the deepwater fold and thrust belts of the Niger Delta. American Association of Petroleum Geologists Bulletin 89, 753 – 780. https://doi.org/10.1306/02170504074.

Crutchley, G.J., Klaeschen, D., Planert, L., Bialas, J., Berndt, C., Papenberg, C., Hensen, C., Hornbach, M.J., Krastel, S. & Brueckmann, W. 2014. The impact of fluid advection on gas hydrate stability: Investigations at sites of methane seepage offshore Costa Rica, Earth and Planetary Science Letters,401,95-109, https://doi.org/10.1016/j.epsl.2014.05.045.

Cunningham, R. & Lindholm, R.M. 2000. Seismic Evidence for Widespread Gas Hydrate Formation, Offshore West Africa. In: Mello, M.R. and Katz, B.J. (eds.) Petroleum systems of South Atlantic margins. American Association of Petroleum Geologists Memoir, 73, 93-105. https://doi.org/10.1306/M73705C8

Daigle, H. & Dugan, B. 2011. Capillary controls on methane hydrate distribution and fracturing in advective systems, Geochemistry Geophysics Geosystem, 12 (1), Q01003, https://doi.org/10.1029/2010GC003392

Davy, B., Pecher, I., Wood, R., Carter, L. & Gohl, K. 2010. Gas escape features off New Zealand: Evidence of massive release of methane from hydrates, Geophysical Research Letters, 37, L21309, https://doi.org/10.1029/2010GL045184

Dickens, G. R. 2003. Rethinking the global carbon cycle with a large, dynamic and microbially mediated gas hydrate capacitor. Earth and Planetary Science Letters. 213 (3-4), 169–183. https://doi.org/10.1016/S0012-821X(03)00325-X

Doust, H. & Omatsola, E. 1990. Niger Delta, in J. D Edwards, and P.A. Santogrossi, eds. Divergent/passive margins basins: American Association of Petroleum Geologists Memoir 48, 201-238. https://doi.org/10.1306/M48508C4.

Foucher, J. P., Nouzé, H. & Henry, P. 2002. Observation and tentative interpretation of a double BSR on the Nankai slope. Marine Geology, 187, 161-175. https://doi.org/10.1016/S0025-3227(02)00264-5

Frankl, E. J. & Cordry, E. A. 1967. The Niger Delta oil Province: Recent development, onshore and offshore. Mexico

City. Seventh World Petroleum Congress Proceedings 2, 195-209. https://doi.org/10.1306/5D25B843-16C1-11D7-8645000102C1865D .

Geletti, R. & Busetti, M. 2011, A double bottom simulating reflector in the western Ross Sea, Antarctica, Journal of Geophysical Research., 116, B04101, https://doi.org/10.1029/2010JB007864 .

Haacke, R.R., Hyndman, R.D., Park, K-P., Yoo, D-G., Stoian, I. & Schmidt, U. 2009. Migration and venting of deep gases into the ocean through hydrate-choked chimneys offshore Korea. GEOLOGY, Geological Society of America, 37(6), 531–534, http://dx.doi.org/10.1130/G25681A.1

Holder, G. D., Malone, R. D. & Lawson, W. F. 1987. Effects of Gas Composition and Geothermal Properties on the Thickness and Depth of Natural-Gas-Hydrate Zones. Journal of Petroleum Technology, 39 (09), 1147–1152. https://doi.org/10.2118/13595-PA

Hovland, M., Gallagher, J., Clennell, M. & Lekvam, K. 1997. Gas hydrate and free gas volumes in marine sediments: Example from the Niger Delta front. Marine and Petroleum Geology, 14, 245-255. https://doi.org/10.1016/S0264-8172(97)00012-3

Hyndman, R. D. & Davis, E. E. 1992. A mechanism for the formation of methane hydrate and seafloor bottom-simulating reflectors by vertical fluid expulsion. Journal of Geophysical Research, 97(B5), 7025–7041. https://doi.org/10.1029/91JB03061

Kessler, J. 2014. Seafloor methane: Atlantic bubble bath. Nature Geoscience, 7 (9), 625–626. https://doi.org/10.1038/ngeo2238

Kroeger, K.F., Crutchley, G.J. and Pecher, I.A. 2023. Slow response of the gas hydrate system to ridge erosion and sea-level rise: Insights from double BSRs on the southern Hikurangi margin (New Zealand) Earth and Planetary Science Letters 624, 118433 https://doi.org/10.1016/j.epsl.2023.118433

Lehner, P. & De Ruiter, P.A.C. 1977. Structural History of Atlantic Margin of Africa: American Association of Petroleum Geologists Bulletin 61, 961-981. https://doi.org/10.1306/C1EA43B0-16C9-11D7-8645000102C1865D .

Maloney, D., Davies, R., Imber, J., Higgins, S. & King, S., 2010. New insights into deformation mechanisms in the gravitationally driven Niger Delta deep-water fold and thrust belt. American Association of Petroleum Geologists Bulletin 94, 1401–1424. https://doi.org/10.1306/01051009080 .

Matsumoto, R., Masuda, M., Foucher, J., Tokuyama, H., Ashi, J. & Tomaru, H. 2000. Double BSR in the Eastern Nankai Trough: fact or artifact. Western Pacific Geophysics Meeting, 2000, American Geophysical Union. http://www.agu.org/meetings/waiswp00.html

McGinnis, D. F., Greinert, J., Artemov, Y., Beaubien, S. E. & Wüest, A. 2006. Fate of rising methane bubbles in stratified waters: how much methane reaches the atmosphere? Journal of Geophysical Research: Oceans 111, C09007. https://doi.org/10.1029/2005JC003183

Minshull, T. & White, R. 1989. Sediment compaction and fluid migration in the Makran accretionary prism. Journal of Geophysical Research, 94(B6), 7387–7402. https://doi.org/10.1029/JB094iB06p07387

Nwachukwu, J. I. & Chukwura, P. I. 1986. Organic matter of Agbada Formation, Niger Delta, Nigeria. American Association of Petroleum Geologist Bulletin 70, 48-55.

Paganoni, M., Cartwright, J. A. Foschi, M., Shipp, R. C. & Van Rensbergen, P. 2016. Structure II gas hydrates found below the bottom-simulating reflector. Geophysical Research Letters. 43, https://doi.org/10.1002/2016GL069452 .

Pecher, I. A., Henrys, S. A., Wood, W. T., Kukowski, N., Crutchley, G. J., Fohrmann, M., Kilner, J., Senger, K., Gorman, A. R., Coffin, R. B., Grenert, J. & Faure, K. 2010. Focussed fluid flow on the Hikurangi Margin, New Zealand—Evidence from possible local upwarping of the base of gas hydrate stability. Marine Geology, 272(1–4), 99–113. https://doi.org/10.1016/j.margeo.2009.10.006

Pecher, I. A., Villinger, H., Kaul, N., Crutchley, G. J., Mountjoy, J. J., Huhn, K., Kukowski, N., Henrys, S. A., Rose, P. S. & Coffin, R. B. 2017. A fluid pulse on the Hikurangi subduction margin: Evidence from a heat flux transect across the upper limit of gas hydrate stability. Geophysical Research Letters, 44, 12385–12395. https://doi.org/10.1002/2017GL076368

Popescu, I., Marc De Batist, B., Lericolais, G., Nouzé, H., Poort, Jeffrey., Panin, N., Versteeg, W. & Gillet, H. 2006. Multiple bottom-simulating reflections in the Black Sea: Potential proxies of past climate conditions. Marine Geology 227, 163 – 176. https://doi.org/10.1016/j.margeo.2005.12.006 .

Posewang, J. & Mienert, J. 1999. The enigma of double BSRs: indicators for changes in the hydrate stability field? Geo-Marine Letters 19, 157-163.

Reijers, T. J. A., 2011. Stratigraphy and sedimentology of the Niger Delta. Geologos17, 133 – 162. https://doi.org/10.2478/v10118-011-0008-3 .

Riboulot, V., Ker, S., Sultan, N., Thomas, Y., Marsset, B., Scalabrin, C., Ruffine, L., Boulart, C. & Ion, G. 2018. Freshwater lake to salt-water sea causing widespread hydrate dissociation in the Black Sea. Nature Communications, 9:117, doi: 10.1038/s41467-017-02271-z |

Ruffine, L., Caprais, J. C., Bayon, G., Riboulot, V., Donval, J. P., Etoubleau, J., Birot, D., Pignet, P., Rongemaille, E., Chazallon, B., Grimaud, S., Adamy, J., Charlou, J. L. & Voisset, M. 2013. Investigation on the geochemical dynamics of a hydrate-bearing pockmark in the Niger Delta. Marine and Petroleum Geology 43, 297-309. https://doi.org/10.1016/j.marpetgeo.2013.01.008

Ruppel, C. 2000. Thermal state of the gas hydrate reservoir; in M. D. Max (eds) Natural Gas Hydrate in Oceanic and Permafrost Environments, Kluwer, Dordrecht. 29–42, https://doi.org/10.1007/978-94-011-4387-5_4

Sahota, J. T. S., 2006. Deepwater Exploration In The NW Niger Delta: Are There Parallels For Indian Exploration? 6th

International Conference and Exposition on Petroleum Geophysics. Kolkata, India, Proceedings, P1387. https://spgindia.org/conference/6thconf_kolkata06/252.pdf

Short, K. C. & Stauble, A. J. 1967. Outline of geology of Niger Delta. American Association of Petroleum Geologist Bulletin 51, 761-799. https://doi.org/10.1306/5D25C0CF-16C1-11D7-8645000102C1865D .

Sloan, D. E. (Jr), 2003. Fundamental principles and applications of natural gas hydrates. Nature, 426, 253-259. https://doi.org/10.1038/nature02135 .

Sloan, D. E.(Jr) & Koh. C., 2007. Clathrate Hydrates of Natural Gases. 3rd Edition. CRC Press. Boca Raton. https://doi.org/10.1201/9781420008494

Solomon, E. A., Kastner, M., MacDonald, I. R. & Leifer, I. 2009. Considerable methane fluxes to the atmosphere from hydrocarbon seeps in the Gulf of Mexico. Nature Geoscience. 2, 561–565. https://doi.org/10.1038/ngeo574

Sultan, N., Voisset, M., Marsset, T., Vernant, A.-M., Cauquil, E., Colliat, J. & Curinier, V. 2007. Detection of free gas and gas hydrate based on 3D seismic data and cone penetration testing: An example from the Nigerian Continental Slope. Marine Geology, 240, 235-255. https://doi.org/10.1016/j.margeo.2007.02.012

Sultan, N., Marsset, B., Ker, S., Marsset, T., Voisset, M., Vernant, A.M., Bayon, G., Cauquil, E., Adamy, J., Colliat, J.L. & Drapeau, D. 2010. Hydrate dissolution as a potential mechanism for pockmark formation in the Niger Delta. Journal of Geophysical Research: Solid Earth, 115, B08101. https://doi.org/10.1029/2010JB007453

Sultan, N., Riboulot, V., Ker, S., Marsset, B., Geli, L., Tary, J.-B., Klingelhoefer, F., Voisset, M., Lanfumey, V. & Colliat, J.-L. 2011. Dynamics of fault-fluid-hydrate system around a shale-cored anticline in deepwater Nigeria. Journal of Geophysical Research: Solid Earth, 116, B12110. https://doi.org/10.1029/2011JB008218

Taladay, K., Boston, B. & Moore, G. 2017. Gas-in-place estimate for potential gas hydrate concentrated zone in the Kumano Basin, Nankai Trough Forearc, Japan. Energies, 10(10), 1552. https://doi.org/10.3390/en10101552

Tinivella, U. & Giustiniani, M. 2013. Variations in BSR depth due to gas hydrate stability versus pore pressure. Global and Planetary Change, 100, 119–128. https://doi.org/10.1016/j.gloplacha.2012.10.012

Tréhu, A. M., Long, P. E., Torres, M. E., Bohrmann, G. R. R. F., Rack, F. R., Collett, T. S., Goldberg, D. S., Milkov, A. V., Riedel, M., Schultheiss, P., Bangs, N. L., Barr, S. R., Borowski, W. S., Claypool., G. E., Delwiche, M. E., Dickens, G. R., Gracia, E., Guerin, G., Holland, M., Johnson, J. E., Lee, Y.-J., Liu, C.-S., Su, X., Teichert, B., Tomaru, H., Vanneste, M., Watanabe, M. & Weinberger, J. L. 2004. Three-dimensional distribution of gas hydrate beneath southern Hydrate Ridge: Constraints from ODP Leg 204. Earth and Planetary Science Letters, 222(3–4), 845–862. https://doi.org/10.1016/j.epsl.2004.03.035

Tuttle, M. L. W., Charpentier, R. R. & Brownfield, M. E. 1999. The Niger Delta Petroleum System: Niger Delta Province, Nigeria, Cameroon, and Equatorial Guinea, Africa. US Geological Survey Open-File Report 99-50-H, Denver, Colorado, P.70. https://doi.org/10.3133/ofr9950H .

Valentine, D. L., Blanton, D. C., Reeburgh, W. S. & Kastner, M. 2001. Water column methane oxidation adjacent to an area of active hydrate dissociation, Eel River Basin. Geochimica et Cosmochimica Acta, 65 (16), 2633–2640. http://dx.doi.org/10.1016/S0016-7037(01)00625-1

Weber, K. J. & Daukoru, E. 1975. Petroleum Geology of the Niger Delta, Tokyo. 9th World Petroleum Congress Proceedings 2, 209-211.

Whiteman, A., 1982. Nigeria –Its petroleum geology, resources and potential, First edition. Graham and Trotman, London. https://doi.org/10.1007/978-94-009-7361-9 .

Wu, S. & Bally, A. W. 2000. Slope tectonics - Comparisons and contrasts of structural styles of salt and shale tectonics of the Northern Gulf of Mexico with shale tectonics of Offshore Nigeria in Gulf of Guinea, in: Mohriak, W., Talwani, M., (Eds.), Atlantic Rifts and Continental Margins - Geophysical Monograph, American Geophysical Union, Washington DC. 115, 151-172. https://doi.org/10.1029/GM115p0151 .

Zander, T., Haeckel, M., Berndt, C., Chi, W-C., Klaucke, I., Bialas, J., Klaeschen, D., Koch, S. & Atgin, O. 2017. On the origin of multiple BSRs in the Danube deep-sea fan, Black Sea, Earth and Planetary Science Letters, 462, 15-25, ISSN 0012-821X, https://doi.org/10.1016/j.epsl.2017.01.006